INTERNATIONAL JOURNAL OF CONSERVATION SCIENCE
ISSN: 2067-533X Volume 15, Issue 4, 2024: 1713-1730 www.ijcs.ro
DOI: 10.36868/IJCS.2024.04.09

3D MODELLING OF THE SVETOVID STATUE FROM ZBRUCZ BASED ON OF INTEGRATED PHOTOGRAMMETRIC AND LASER DATA

Sylwia BRYNDZA[1], Urszula MARMOL[2,*], Natalia BOROWIEC[2]

[1] Quasar, Inc., Łomianki, Poland
[2] AGH University, Faculty of Geo-Data Science, Geodesy and Environmental Engineering, Krakow, Poland

Abstract

The theme of the paper is the preparation of a 3D model of the stone sculpture of Svetovid from Zbrucz, using integrated data, derived from two measurement technologies – close-range photogrammetry and terrestrial laser scanning. The research also focused on comparing the obtained products and the created models, to best represent the measured object. The emphasis was on the quantitative and qualitative analysis of the results obtained. The presented analyses focused on factors affecting the quality of the final product. The research aimed to compare the two methods, evaluate the integration process and develop the best possible 3D model of the statue. The analyses carried out based on the collected data show many advantages of the integration process. The image and laser data have different properties, typical of each measurement method. Photogrammetric data allows better identification of edges and fine details, which is important for sculpture with complex geometry. Laser data, on the other hand, allows the acquisition of accurate spatial information for homogeneous areas and provides direct metric information. A comparison of the similarities and differences in point clouds and models highlights the fact that to create a model of an object, it is necessary to define an adequate data acquisition and processing, depending on the purpose of the model being created.

***Keywords**: 3D modelling; Photogrammetry; Terrestrial laser scanning: Accuracy analysis*

Introduction

Remote object inventory is to determine the shape, dimensions and location of an object, as well as other features extracted from the analysis of photogrammetric and laser data. The term also refers to heritage protection, where it means „the representation of the appearance of a monument in an image or descriptive form" [1]. According to this definition [1], an inventory can be distinguished:

- measuring - scale drawings prepared based on direct measurement;
- surveying - drawings of a monument, a historic complex or a monument with its surroundings drawn to scale based on a measurement made with surveying instruments;
- photogrammetric;
- photographic - a set of photographs taken at one time giving an idea of the monument (in the case of architectural monument also of its interior) and of all its details;
- dendrological - survey inventory with marked trees and shrubs with the designation of their species, height, the largest diameter of the crown;

* Corresponding author: entice@agh.edu.pl

- descriptive - description of the monument prepared according to the adopted scheme adapted to the type of the monument, using the terminology accepted in heritage studies.

Among the modern survey techniques used in cultural heritage inventory and research, photogrammetry and laser scanning should undoubtedly be mentioned.

These methods offer great potential, revolutionising many activities in heritage conservation [2]. Photogrammetry and scanning are part of a range of non-invasive methods, outlining a new dimension of survey and analytical work on monuments, which therefore require a reformulation or refinement of existing methodology for field work. These techniques, referred to as indirect measurement methods, allow for the accurate representation of irregularly shaped objects or objects with rich ornamentation, details or defects. Currently, these methods represent the optimum way to obtain documentation of the existing condition of heritage objects in terms of accuracy, quality and cost [3].

One of the goals of object inventories is to perform 3D modelling. Because of the 3D model obtained, it is possible to measure the shape and position, to prepare documentation and to reconstruct the heritage object in the case of its destruction. There are determinants that define the purposes that digital documentation should fulfil. Nowadays, it should:

- involve the capture of 3D data (4D if possible) from many sources, having different resolutions and presenting different content,
- include the management and maintenance of the resulting 3D (4D) models for further applications,
- provide the ability to visualise and present the results to distribute the information and enable data search via Internet or in databases,
- enable the digital inventory and sharing of data for educational, research, conservation, entertainment or tourism purposes [4].

Terrestrial data is often acquired by integrating image data from high-resolution cameras and spatial clouds with TLS [5]. The integration of measurement techniques makes it possible to compensate for some errors and acquire missing data due to the technical limitations of the instruments used, as well as to create a product that was previously unachievable. This procedure is used to obtain high accuracy models that can be used to study shape, geometric relationships or positioning in three-dimensional space [6].

The use of different sources to collect data implies that certain factors need to be considered in the process, such as how and when the data was collected and the purpose of the study. Integrating data also imposes the need to determine a common georeference. The resulting point clouds vary from one method to another and this makes them difficult to merge and align.

The cloud, derived from scanning, represents point data that, in addition to coordinates, also has information about RGB values or intensity. The measurement takes place at a stationary location and the products can be processed by filtering, searching, edging or classification. Photogrammetry, on the other hand, provides raster data, which requires knowledge of internal and external orientation elements to determine the coordinates of points. The processing of images into 3D products is enabled by matching procedures. In order to determine the georeference, a single external reference system has to be adopted and the individual systems in which the data was acquired have to be aligned with each other [6].

Review of the literature

The inventory of architectural and archaeological objects with integrated photogrammetric and laser data is a highly current topic that has been discussed in many scientific publications.

The paper [7] aims to validate close-range Structure from Motion (SfM) for heritage by analysing the point density and the 3D mesh geometry in comparison with TLS. In [8] the potentials in using 3D modelling as a tool of investigation and visualization for a deeper understanding of archaeological sites is presented. The discussion is supported by the case study of the roman villa of Aiano, built at the beginning of the 4th century A.D. and characterized by monumental architecture and decorations. The final result of study [9] is a 3D model of Halmyris Citadel (Murighiol, Tulcea County), which can be used to help preserving the archaeological site and serve as a base for future on-site restoration works. In the paper [10], the authors discuss a new methodology that combines the advantages of computer vision photogrammetry with those of laser scanning by applying the photographic textures produced with photogrammetry to the geometric data obtained from laser scanning. The authors conclude that their method allows archaeologists to achieve the best possible fidelity 3D models for interpretation and study. The aim of the paper [11] is to identify a suitable pipeline in order to build high-resolution 3D models and 2D orthophotos of objects and architectural structures of particular historical and cultural importance by means of the photogrammetric method. This work describes a simple procedure for the definition of such projection direction, while also enabling the express the object position according to certain specific requirements. In addition, the use of low-cost Smartphone and action cameras was investigated to conduct photogrammetric surveys. In the publication [12] the hybrid model of historical and modern data will be used for archaeological interpretations of the excavation. As first results, point clouds calculated by Structure from Motion and the orientation of historical images in relation to the modern 3D model using direct linear transformation are shown. In the study [13], Kızılkoyun Necropolis was first scanned with a laser scanner and then with the unmanned aerial vehicle (UAV), photogrammetric products have been produced. The result of the evaluation is a surface model of the rock tombs in the region and some archaeological figures and structures have been transferred to the digital environment. Methodology presented in the paper [14] was based on combination of novel techniques such as UAV photogrammetry and HBIM modelling and by leveraging additional information derived from common representation methods. The main idea was to create a low-cost workflow in complex conditions. The project [15] will be carried out in the autonomous Iraqi region of Kurdistan. During several expeditions to this region, a big amount of scientific material has been collected. A part of this is a contribution of the CTU, which is focused on geomatics technologies, which means photogrammetric documentation of whole localities and detailed terrestrial photogrammetric modelling of objects and findings. In the study [16], theodolite, sextant and graphometer instruments on display at the Istanbul Technical University (ITU) were modelled using photogrammetric and laser scanning methods. To compare the accuracy of the models, calliper measurements were taken from specific points of the instruments used in the modelling. In the article [17], a cultural heritage located in Mersin was modelled in 3D using an unmanned aerial vehicle (UAV). Circular mission plan in the mobile phone application was preferred. Digital surface model, orthophoto and 3D model of Ucayak Ruins have been created. The case studies [18] are representative of specific situations in which archaeology requires digitization of artefacts. The first one concerns the Temple of Apollo in Gortyn, the second one is the ancient city of Nora and the third one is the Museo Civico of Eremitani in Padua. The paper explains how 3D metric surveying has served for the representation and analysis of stratigraphic sections of buildings in the case of the Gortyn site, for the creation of virtual tours of archaeological sites in the case of Nora and for the documentation and visualization of small artefacts in the case of the Museo Civico of Eremitani by highlighting potentials and criticalities of the method. The research [19] used medium and close-range type of laser scanners to digitally record the heritage objects. The aim of this research was to develop methodology framework for digital recording and 3D reproduction of archaeological artefact and heritage sites in Malaysia by using terrestrial laser scanning technology. The article [20] describes a hybrid approach combining photogrammetry and laser scanning for 3D documentation of Qasr Al-Abidit palace; a rare example of Hellenistic architecture in Jordan. During data collection the information on edges and linear surface features is based on the analysis of images, whereas information on object geometry is provided from the laser data. By the combination of both data sources, the shape of 3D features has been determined. In the paper [21], authors discuss the steps required to homogenize the information and the methods used to perform block alignment in photogrammetric cases. A study of low-altitude aerial photogrammetry with several cameras and platforms is presented for the Roman camp of A Cidadela in NW Spain as a representative example of an archaeological site that is difficult to survey using a single photogrammetric platform. The paper [22] studies the potential of the recent entry-level phone camera for performing close-range photogrammetry as an affordable abundant tool. To achieve this goal, Marinid Royal Necropolis from the UNESCO heritage city of Fez in Morocco was photographed and 3D modelled using a Smartphone and a DSLR camera. The study [23] focuses on using a combination of terrestrial laser scanning and UAV photogrammetry to establish a three-dimensional model and the associated digital documentation of the Magoksa Temple, Republic of Korea. Herein, terrestrial laser scanning and UAV photogrammetry was used to acquire the perpendicular geometry of the buildings and sites, where UAV photogrammetry yielded higher planar data acquisition rate in upper zones, such as the roof of a building, than terrestrial laser scanning. Authors [24] present an innovative low-cost system that allows high quality and detailed reconstructions of indoor complex scenarios with unfavourable lighting conditions by means of close-range nadir and oblique images as an alternative to drone acquisitions. The paper [25] aims to find a more appropriate method and setting for 3D model photogrammetric reconstruction of human remains, demonstrating the importance of this digital technology for the study of poorly preserved osteo-archaeological remains. For these purposes, the results obtained using two different settings for image acquisition (one with macro and one with standard lens) were compared and discussed. In the research [26] the specific methodology was applied to produce a scale 3D model of Arutela Roman Castrum in a digital environment. A complex product is created, with complemental geometry and texture. The accurate geometry and appearance details (size, shape, position and texture) can be used for a proper documentation, preservation and restoration applications.

As can be seen from the above literature review, the authors have used photogrammetric and laser technologies in modelling and inventorying archaeological sites with great success. The data obtained from photogrammetry and scanning are complementary to each other - the imperfections of one method are compensated for by the advantages of the other, resulting in an optimal final product.

Experimental part

Characteristics of the object

The subject of this study is the stone sculpture Svetovid from Zbrucz, located near Wawel Cathedral on the side of Grodzka Street in Krakow (Fig. 1). It is a replica of a limestone sculpture located in the Archaeological Museum in Krakow and featured in the museum's logo. The original sculpture is one of the museum's most valuable exhibits. The statue, dated to the 10th century or the turn of the 10^{th} century, was found in 1848 in the Zbrucz River in Ukraine and given to Count Mieczysław Potocki, who then donated it to the Krakow Scientific Society. In 1851, the statue was exhibited in the hall of the Jagiellonian Library and at the turn of 1858/1859 it found its way to the Exhibition of Antiquities and has been in the museum's collection ever since. At that time, the Svetovid motif often appeared in Polish culture, presenting a variety of forms and a wide range of meanings and nowadays it is an icon of neo-pagan religious groups [27, 28].

The statue of Svetovid is a 35cm wide quadrilateral stone pillar. It is situated on a platform 80cm wide and the whole object is about 3m high. Near the measured object is an extensive tree, which is a natural monument. The sides of the sculpture present figural representations and it is topped by a „hat”, covering four linked human heads. The walls feature three horizontal bands separated by mouldings, illustrating the creator's conviction about the world around him. Below the four-headed demigod, equipped with elements such as a horn, ring, sabre and horse, there is a strip referring to the earth and the whole is supported by a three-headed figure identified with the lord of the underworld. This sculpture stands out from other Slavic statues, which usually presented only one „floor” of the cosmos, rather than the entire universe [28].

Fig. 1. Svetovid statue from Zbrucz (a), four sides of Svetovid (b) [28]

Data acquisition

Acquisition of spatial information about the study object started with a terrestrial laser scanning with Z+F Imager 5010C scanner. In the initial field view, the specifications of the object and its location were familiarised, which made it possible to define difficult locations for measurement and improved the measurement process. In order to obtain a complete view of the monument, four scanner positions were established at the corners of the monument. A nearby tree made it impossible to place them at an equal distance around the object, so position no.4 was located in close proximity to it.

The point cloud was acquired with a high angular resolution setting providing 10,000 points/360° and normal quality. In addition, the option to take images was set in the scanner.

The scanning was followed by the acquisition of the data required for photogrammetric processing using a Nikon D5200 camera. Photographing the object was preceded by preparing the camera for measurement. The focal length was set to the minimum value of 18mm. The object was photographed from all sides to obtain the best possible overlap and to capture all details. Images were taken at a fixed focal length. The use of flash was avoided and it was checked that the subject was not blurred in the photographs. Images were taken in portrait orientation, which allowed the entire statue to be framed in one image. A total of 76 images of the object were acquired in JPG format. The nearby tree, previously mentioned, made it impossible to accurately photograph one side of the statue.

Terrestrial laser scanning

The data processing, acquired by terrestrial laser scanning, has started with the merging of point clouds in Autodesk ReCap Pro. Four scans were loaded into the software. The registration of the clouds was carried out automatically. A scan that had not been merged was then attached to the registered group. This cloud was attached based on the manual identification of three tie points located in the surroundings of the surveyed object. The registration report is shown in Table 1.

Table 1. Autodesk ReCap scan registration report

Scan number	overlap (%)	balance (%)	points < 6mm (%)
1	24,1	56,2	72,9
2	43,3	21,3	85,9
3	40,4	6,3	88,5
4	16,8	33,0	92,2

The merged scans were limited to the area that included the study object and then the redundant information created by capturing the entire scene was removed. The final result is shown in Figure 2.

Fig. 2. Point cloud views created by combining all four scans. Object shown from two sides

The accuracy of the scan merging was also checked and some discrepancies were found. A limited point cloud was loaded into CloudCompare to improve scan registration. The scans were matched using the point cloud alignment tool based on the indication of corresponding point pairs. The mean square error of this fit was 2.4cm. The registration of the scans was then corrected by an automated method using the ICP algorithm. After this alignment, the RMS decreased to 0.5cm.

Photogrammetry

The acquired images were processed in Agisoft Metashape Professional. In the first step, image alignment was carried out. The result of this process is a sparse point cloud and the estimated coordinates of the camera projection centres (Fig. 3). The averaged resolution for all aligned images was 0.5mm/pix.

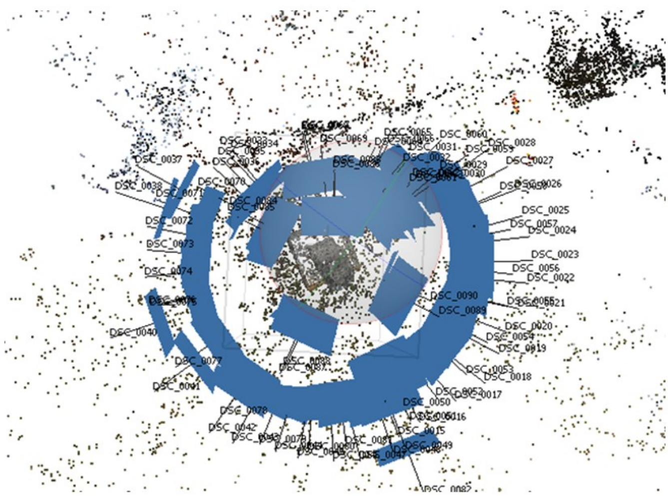

Fig. 3. Sparse point cloud and determined positions of camera projection centres

In the next stage of the work, the study area was limited and a dense, high-quality point cloud was generated. The moderate option was selected as the algorithm for calculating the depth maps, allowing for optimal filtering of incorrect measurements from the point cloud. The option to extract data with the colour parameter was then selected in the tool settings. The created cloud was cleared of points representing surrounding elements and noise present in the upper part of the object. The final cloud from the photogrammetric processing is visualised in Figure 4.

Fig. 4. Dense point cloud of the study object

Integration of photogrammetric and laser data

The processing of the measurement data resulted in two dense point clouds, generated from the photogrammetric and laser data. The integration in the above study consisted of positioning the photogrammetric cloud in the scanner system to give it the appropriate dimensions and merging the two clouds. This step was necessary to obtain a complete metric product. The next step was to generate mesh models and textured models.

The mesh models were generated in Agisoft Metashape in three variations. Firstly, separate models were created based on the photogrammetric and laser point cloud and then on the point cloud created from the integration of the two above. A mesh model was generated for each variant, based on the dense point cloud. In the tool parameters, an arbitrary type of surface was selected, suitable for three-dimensional models of closed objects such as statues or buildings, with a high number of polygons created in the final mesh. In the advanced parameters, the possibility to perform interpolation was set, allowing areas not covered by points to be filled and the possibility to calculate the colours of the vertices of the mesh.

Subsequently, diffuse map textures were created for each of the above models from the images. A generic mapping mode was selected in the tool parameters, as well as a mosaic mode for merging the colours of the pixels from the different cameras into the final texture. The generated mesh models and texture models were at a later stage submitted to qualitative analysis.

Quantitative result analysis

Analysis of measurement noise

Measurement noise is one of the sources of random errors impacting on the quality of results important for geometric analysis. The reasons for its occurrence may be due to errors in measurement technology or adverse effects of the external environment, as well as the distance of the measured surface and its reflectivity. The appearance of noise can result in artefacts or significant deviations from the reference surface visible in the cross-section [29].

The magnitude of the noise, appearing in the dense point clouds obtained by photogrammetric and laser processing, was determined based on several study areas differing in the nature of the study surface. Analyses were carried out for flat surfaces and surfaces with two depth differences.

Firstly, the noise existing on a flat horizontal and vertical surface was investigated. For this purpose, a fragment of the platform on which the sculpture is located (horizontal surface) and a fragment of the information plate, located at the bottom of the sculpture (vertical surface), were selected from the point cloud. These areas, extracted from the point cloud using the *Cross Section* tool, are highlighted in Figure 5.

Fig. 5. Flat object fragments selected for measurement noise testing

Planes were fitted into the extracted parts and, in sequence, distances were determined from them for each point in the cloud using the *Compute Cloud to Mesh Distance (C2M)* tool. Next, filtering was carried out using the *Noise filter* tool available in the software. This algorithm uses the distance from the local surface. It works by fitting a plane around each point of the cloud and then removing points if their distance exceeds an acceptable distance. The algorithm is similar to low-pass filtering and gives good results when filtering flat surfaces. The result of the filtering depends on the method chosen by the user to estimate the local underlying surfaces (based on the number of neighbouring points or on the value of the radius of the sphere) [30]. Table 2 compares the results obtained for the data before and after filtering.

Table 2. Comparison of measurement noise for flat surfaces

Surface		***Horizontal***				***Vertical***			
Technology		Photogrammetry		Scanning		Photogrammetry		Scanning	
Noise filtration		no	yes	no	yes	no	yes	no	yes
Number of points		35 762	12 441	1 743	1 034	10 121	5 339	621	355
Percentage of filtered points		-	65%	-	41%	-	47%	-	43%
RMS of plane fit [mm]		0.5		0.9		0.2		0.7	
Distance from plane [mm]	**Max**	2.1	1.9	4.6	2.6	0.9	0.8	2.5	1.3
	Mean	0	0	0	0	0	0	0	0
	σ	0.5	0.5	0.9	0.5	0.2	0.2	0.7	0.3

In the considered example, the horizontal surface is not perfectly flat, it has real ridges, therefore there are, greater deviations from the plane than for the vertical surface. In both cases, in the laser data, the calculated distances from the plane are larger than for photogrammetric data, with the result that they may be less accurate and noisier. However, the difference is not that significant, its value for the vertical surface is about 1.6mm. The noise filtering carried out does not significantly change the distances determined from the photogrammetric data, but it is noticeable in the laser data and the maximum difference in value is about 2mm. This is the value for a horizontal surface. This means that there is no significant measurement noise in the products in the case of flat surfaces, but that the surfaces more accurately represent the image data. Test area plots of the flat vertical surface, showing the results of the analyses, are presented in Figure 6.

The second performed analysis, concerning flat surfaces and the measurement noise present in them, was the determination of the distances between point clouds acquired using the two measurement technologies. These distances were calculated for scanning data due to its lower density using the *Compute Cloud to Cloud Distance (C2C)* tool. The study was carried out using the input data and the data processed with the noise filtering tool. Their results are shown in Table 3 and Figure 7.

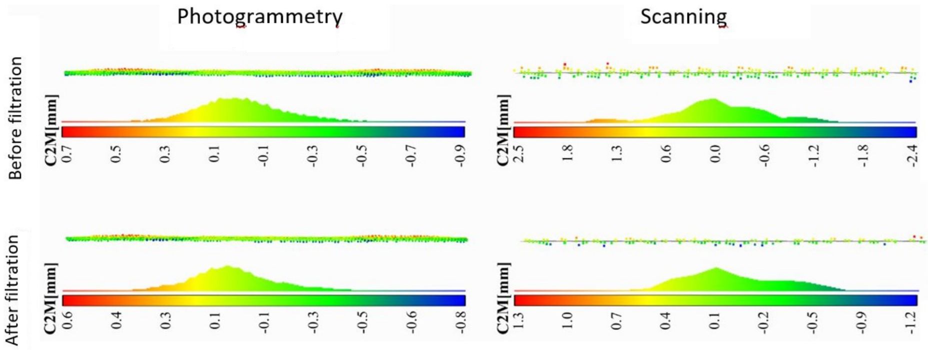

Fig. 6. Comparison of the distance from the fitted plane for a flat vertical surface.

Table 3. Comparison of distances between point clouds for flat surfaces

Surface		***Horizontal***		***Vertical***	
Noise filtration		no	yes	no	yes
Distance [mm]	**Max**	4,7	3,2	4,0	3,0
	Średnia	1,0	1,1	1,3	1,2
	σ	0,7	0,5	0,7	0,6

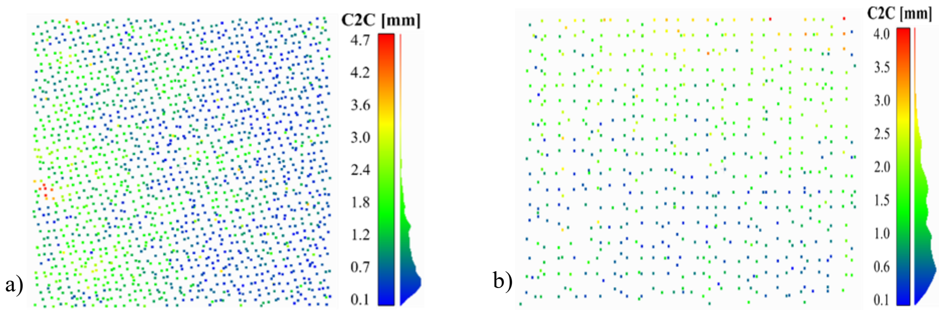

Fig. 7. Distances between point clouds determined for laser data for the study areas before filtering: (a) horizontal surface; (b) vertical surface

In the next stage of the study, surfaces with some depth variations were analysed. These areas are indicated in Figure 8. The middle section of the sculpture, containing the figural representations (Fig. 8a), was chosen as the low-variation fragment and one of the four heads, located in the highest part of the object (Fig. 8b), was chosen as the high-variation fragment.

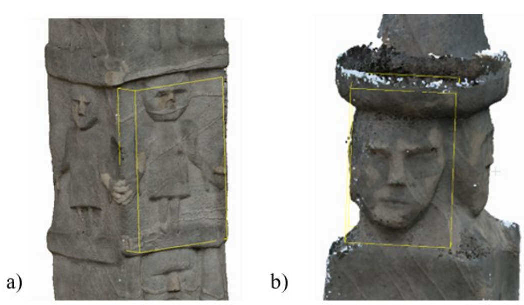

Fig. 8. Surfaces with two depth variations: (a) small depths; (b) large depths

Noise analysis was carried out by determining the differences present in the point clouds and their distances to each other and then by analysing the filtering performed using the tools that were used previously for the study of flat surfaces. The result of the calculated distances between the cloud from photogrammetry and scanning for small depth surface is shown in Figure 9 and, for large depth surface, in Figure 10.

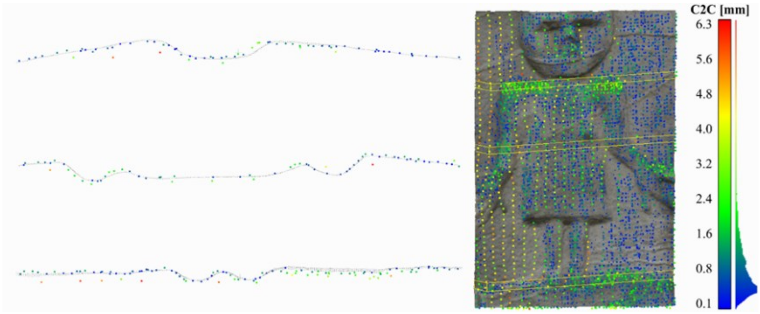

Fig. 9. Distances between point clouds determined for surfaces with small depth differences, together with cross sections determined at three locations

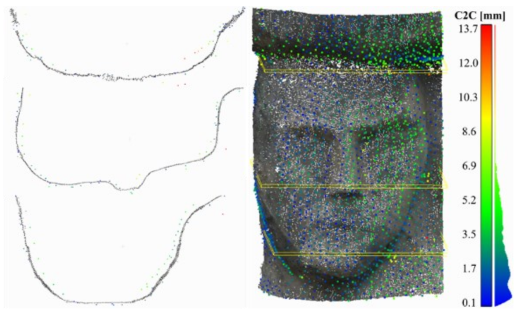

Fig. 10. Distances between point clouds determined for surfaces with large depth differences, together with cross sections determined at three locations

For both selected fragments, the distances are small, most oscillating around 1mm, for the small depth fragment and between 1 and 3mm for the large depth fragment. There are, however, isolated points whose distances between data reach up to 6mm (small depths) and up to 14mm (large depths). These points may indicate the presence of measurement noise, as after filtering the values have decreased especially for the area having large depth differences. The maximum distance difference there decreased by 4mm (Table 4).

Table 4. Comparison of distances between point clouds for surfaces with depth variation

Surface		***Small depths***		***Large depths***	
Technology		Photogrammetry	Scanning	Photogrammetry	Scanning
Number of points		132 581	7 864	130 013	4 273
Number of points after filtration		65 637	4 947	76 109	2 882
Percentage of filtered points		50%	37%	41%	33%
Distance before filtration [mm]	**Max**	6.3		13.7	
	Mean	1.1		2.8	
	σ	0.9		1.9	
Distance after filtration [mm]	**Max**	5.6		10.0	
	Mean	0.9		2.7	
	σ	0.6		1.8	

Edge effect analysis

The high point density in the analysed data allows, not only an accurate representation of the surface, but, also, the modelling of edge lines in vector form. The next analysis performed was a study of the accuracy of edge delineation from laser and photogrammetric data. In the case of laser data, errors can occur at the edges, referred to as the edge effect. The cause of these errors is the refraction of the laser spot at the edges of the object, in which case part of the beam is reflected from the correct surface and the rest from the surface behind it [31].

In order to perform the analysis, two selected edges of the final mesh model were vectorised. These were taken as reference data relative to which the edge effect analysis was performed. These edges were compared with point cloud fragments (Figs. 11 and 12).

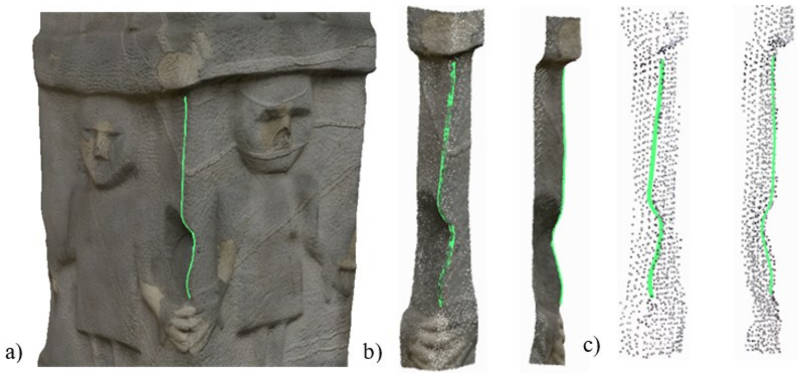

Fig. 11. Comparison of the vertical edge vectorised on the mesh model (a) and superimposed on point clouds from photogrammetric (b) and laser measurements (c) shown from two sides

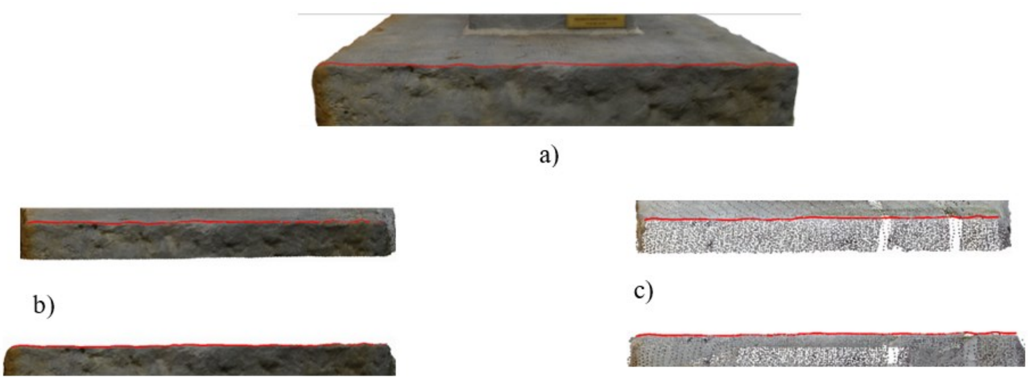

Fig. 12. Comparison of the horizontal edge vectorised on the mesh model (a) and superimposed on point clouds from photogrammetric (b) and laser measurements (c) shown from two sides

The vectorised edges coincide completely with the photogrammetric point cloud which means that the data accurately describes the shape of the object. In the case of laser data, some deviations and blurring of edges and corners can be seen. These may be due to the greater noise of the point cloud and its lower density or may be due to the occurrence of the edge effect mentioned above. This results in a weaker representation and identification of edges, as well as a generalisation of the occurring details and cavities. The surface created from these data is smoother, but the general shape of the object is consistent with the real one.

Qualitative analysis of the results

The qualitative research involved a visual assessment of the resulting products created from point clouds. These clouds were acquired using two measurement technologies and loaded into the Agisoft Metashape software to generate a mesh and a model with textures. The final stage of the study carried out was an analysis of the quality and completeness of the final model made based on selected details of the sculpture.

Visual assessment of mesh models

The first step in the visual assessment of the products was the evaluation of the mesh models. The analysed models were created by processing the photogrammetric and laser point clouds and the data produced by their integration. The evaluation consisted of an analysis of the shape and completeness of the modelled object and the differences present in the models. The solid models generated from the data from the different measurement technologies are shown below (Fig. 13).

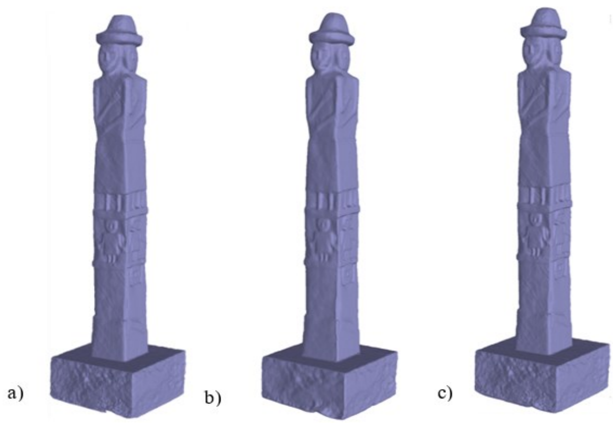

Fig. 13. Comparison of solid mesh models created from photogrammetric (a), laser (b) and integrated photogrammetric and laser data (c)

The models created from the photogrammetric and laser data are similar and have no major defects, but the photogrammetric model more accurately represents the structure of the measured relief. The created mesh models are in line with the quantitative analysis carried out on the original point clouds, which also showed less noise and better density of the photogrammetric cloud and thus better edge identification.

The model created as a result of data integration is close to the photogrammetric model, due to the much higher point density in relation to the scanning cloud. The difference, however, is noticeable in the upper part of the relief, which, due to its height, was not accurately recorded. This is where the model created from the merged data has the smallest gaps, resulting in the best representation of the relief surface (Fig. 14).

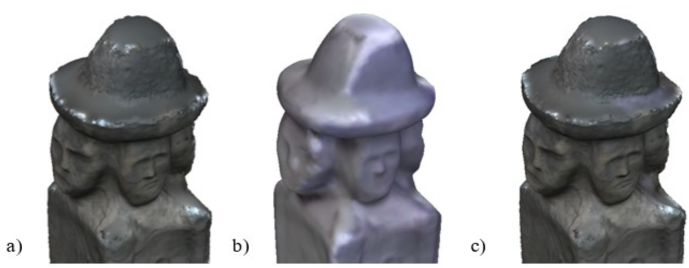

Fig. 14. Comparison of the top mesh models created from: photogrammetric (a), laser (b) and integrated photogrammetric and laser data (c)

The integration of point clouds recorded with two measurement technologies has a positive effect on the final view of the modelled object. Data integration eliminates particular errors, such as inaccuracy of edge mapping for laser data or excessive surface roughness, which characterises photogrammetric data.

Visual evaluation of textured models

Another aspect of the visual assessment was the analysis of the textures generated from the images for each of the three mesh models. Consideration was given to the general quality of the resulting texture, its resolution, completeness and colour compared to the actual appearance of the measured object.

The generated textures for each model accurately reflect the structure and roughness of the surface and correctly reproduce the actual colours of the object. On the walls of the sculpture, all cavities and fine details are clearly visible. The slight differences in the colours of the textures, compared to the real ones, are due to the non-uniform lighting of the object during the measurement, but the created models are satisfactory and visually acceptable. The only inconsistencies appear in the upper part of the sculpture. These are due to the difficulty in capturing these elements in the images taken from the ground (Fig. 15).

Fig. 15. Comparison of final models with textures created from photogrammetric (a), laser (b) and integrated photogrammetric and laser data (c)

Quality assessment of the reproduction of object details

In order to perform a detailed analysis of the final model of the sculpture, a study of the quality of the representation of its details was carried out. This study was performed on several areas presenting important details of the sculpture. These areas present characteristic types of forms and shapes, such as sharp edges, smooth folds, small cavities and bulges and flat surfaces. Verification of the quality and completeness of the presented content on the resulting object model with textures was performed with reference to the original digital images.

The first element examined was a gold plaque, located at the bottom of the measured object, containing information about performed renovation (Fig. 16).

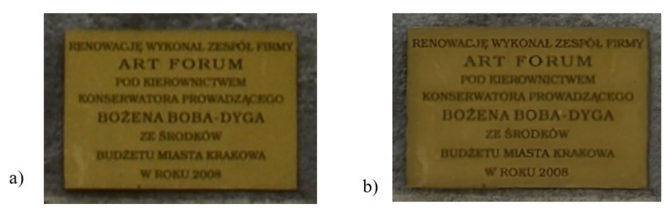

Fig. 16. The information plaque recorded in the photograph (a) and its view on the final model (b)

On the basis of the inscription on the plaque, it is possible to assess the quality of the reproduction of very small elements with large differences in brightness. The plaque is a rectangular shape with actual dimensions of 8 x 12cm and the inscription on it consists of black letters approximately 0.5cm high. This inscription is readable, but the edges of the letters are blurred when approached, compromising the visual quality of the model. In addition, the sharp edges of the study plate also have slight noise visible when zoomed in, which distorts its image in the final product.

The next fragment selected for analysis was the upper part of the sculpture representing one of the four heads of the deity (Fig. 17).

At this place on the real object there are small, but visible differences in the brightness of the material of which it is made. These are also clearly visible on the textured resulting model, which demonstrates its correctness and conformity with the real image. In addition, the model shows correctly reproduced draping, going diagonally and the rough texture of the material.

Further examples show the quality of reproduction of very fine details such as hands (Fig. 18).

a)  b)

Fig. 17. A fragment of the sculpture selected for colour accuracy testing as seen in the photograph (a) and the final model (b)

a) 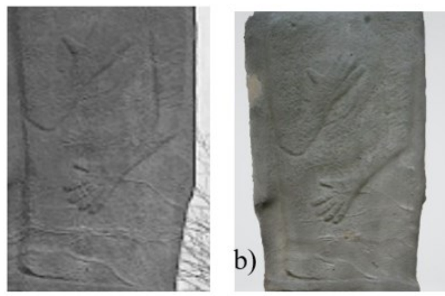 b)

Fig. 18. Comparison of the reproduction quality of the small details of the sculpture in the photograph (a) and the final model (b)

In this case, the hands on the model are represented very clearly. It is possible to distinguish individual fingers and the characteristic cracks and cavities present on the statue can also be seen.

Another example is the depiction of the god-warrior attributes, namely the horse and the sabre (Fig. 19).

a) 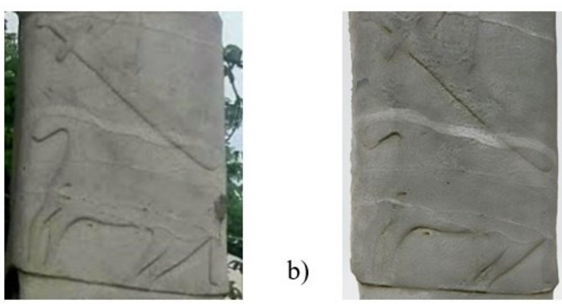 b)

Fig. 19. Comparison of the reproduction quality of the small details of the sculpture in the photograph (a) and the final model (b)

This relief has become blurred and damaged by the passing of years. Nevertheless, it is still readable on the 3D model. Some deformation has occurred to the horse's head, but this is also poorly visible on the original sculpture.

Conclusions

The goal of this paper was to integrate photogrammetric and laser data in the modelling process of an archaeological object and to analyse the accuracy of the obtained results. The activities and studies performed in the study underline the necessity of integrating measurement data for a better geometric and qualitative representation of the measured object. In the study, a method integrating image and laser data was used to provide sufficient data for the documentation of the monument on the example of the Svetovid sculpture from Zbrucz, located in Krakow.

The study object is characterised by the homogeneous structure of the material from which it is made and there are no deviations caused by its reflectivity that could affect the result of the analysis. Noise, which is visible in the data and represents random errors, mainly appears at the edges, in areas of refraction or relief of sculpted elements. The amount of incorrect information is also influenced by the measurement technology. Photogrammetric data more accurately represent the shape of the surface where folds or breaks occur. For flat surfaces, the differences in products from the different technologies are not as evident.

Measurement with a scanner can also cause errors due to edge effects. The 3D model created by the laser scanner contains a large amount of data, representing the surface of the object. However, the higher amount of noise and lower density make the identification of edges, corners and breaks difficult. These edges can only be determined by approximation. In order to improve the visual quality of these details, it is necessary to integrate the data, from the scanner and the images, providing a better representation of such elements.

The next conducted analyses concerned the qualitative evaluation of products created from point clouds. The first of these involved the evaluation of mesh models created using single measurement technologies and a model created from two integrated point clouds. The analysis concluded that the sculpture was best represented by the model generated from the integrated data. This choice was also dictated by the quantitative analysis carried out, which provided information on the quality and accuracy of the individual point clouds. The model is close to the photogrammetric model, but because the point clouds were merged, it was possible to fill in missing parts. The qualitative research also involved evaluating the textures generated from the images. The final textured 3D model presents satisfactory visual quality. Correctly reproduced details, colours and cavities are visible on the model, as well as the complex structure of the sculpture.

The conducted work presents the process of modelling a heritage object on the basis of integrated photogrammetric and laser data. The performed quantitative and qualitative studies of the acquired data show the many advantages of this process. They also indicate that obtaining a reliable model of a cultural heritage object requires a proper process of data acquisition, processing and analysis and evaluation of the final product. The mentioned advantages of the integration process consist in the possibility to compensate for the errors and disadvantages of the individual measurement technologies.

Acknowledgments

The article was prepared under the research subvention of the AGH University of Science and Technology No. 16.16.150.545 in 2024.

References

[1] M. Kurzątkowski, **Mały słownik ochrony zabytków**, Ministerstwo Kultury i Sztuki, Ośrodek Dokumentacji Zabytków, 1989.

[2] R. Zapłata, E. Leonhardt, *Dobra kultury i środowiska-nowe możliwości nieinwazyjnej*

dokumentacji i diagnostyki podczas badań terenowych–idea terenowego laboratorium, **Cyfryzacja w naukach o przeszłości i ochronie zabytków–digitalizacja i nieinwazyjne badanie dziedzictwa kulturowego in situ**, 93. www.academia.edu/38540996/.

[3] A. Boroń, A. Rzonca, A. Wróbel, *Metody fotogrametrii cyfrowej i skanowania laserowego w inwentaryzacji zabytków*, **Roczniki Geomatyki**, **5**(8), 2007, pp. 129–140. www.researchgate.net/publication/318494676.

[4] F. Remondino, A. Rizzi, *Reality-based 3D documentation of natural and cultural heritage sites-techniques, problems and examples*, **Applied Geomatics**, **2**(3), 2010, pp. 85–100. DOI: 10.1007/s12518-010-0025-x.

[5] K. Michałowska, **Modelowanie i wizualizacja danych 3D na podstawie pomiarów fotogrametrycznych i skaningu laserowego**, Rzeszów, Wyższa Szkoła Inżynieryjno-Ekonomiczna z siedzibą w Rzeszowie, 2015. www.researchgate.net/publication/290929636.

[6] J. Markiewicz, *Aspekty integracji danych fotogrametrycznych dla generowania 3D modeli wybranych obiektów przestrzeni miejskiej*, **Archiwum Fotogrametrii, Kartografii i Teledetekcji**, **24**, 2012, pp. 199–209. https://www.researchgate.net/publication/270685341.

[7] J. Moyano, J.E. Nieto-Julián, D. Bienvenido-Huertas, D. Marín-García, *Validation of Close-Range Photogrammetry for Architectural and Archaeological Heritage: Analysis of Point Density and 3D Mesh Geometry*, **Remote Sensing**, **12**(21), 2020, Article Number: 3571. DOI: 10.3390/rs12213571.

[8] D. Ferdani, E. Demetrescu, M. Cavalieri, G. Pace, S. Lenzi, *3D Modelling and Visualization in Field Archaeology. From Survey To Interpretation Of The Past Using Digital Technologies*, **GROMA: Documenting Archaeology**, **4**, 2020. DOI: 10.12977/groma26.

[9] A.V. Tache, I.C.A. Sandu, O.C. Popescu, A.I. Petrisor, *UAV solutions for the protection and management of cultural heritage. Case Study: Halmyris archaeological site*, **International Journal of Conservation Science**, **9**(4), 2018, pp. 795–804. www.researchgate.net/publication/331330890.

[10] C. Dostal, K. Yamafune, *Photogrammetric texture mapping: A method for increasing the Fidelity of 3D models of cultural heritage materials*, **Journal of Archaeological Science: Reports**, **18**, 2018, pp. 430–436. DOI: 10.1016/j.jasrep.2018.01.024.

[11] M. Pepe, D. Costantino, *Techniques, tools, platforms and algorithms in close range photogrammetry in building 3D model and 2D representation of objects and complex architectures*, **Computer-aided Design and Applications**, **18**(1), 2023, pp. 42–65. DOI: 10.14733/cadaps.2021.42-65.

[12] P. Kalinowski, F. Both, T. Luhmann, U. Warnke, *Data fusion of historical photographs with modern 3d data for an archaeological excavation – concept and first results*, **The International Archives of the Photogrammetry, Remote Sensing and Spatial Information Sciences**, XLIII-B2-2, B2-2021, 2021, pp. 571–576. DOI:10.5194/isprs-archives-xliii-b2-2021-571-2021.

[13] H.İ. Şenol, A. Memduhoglu, M. Ulukavak, *Multi instrumental documentation and 3D modelling of an archaeological site: a case study in Kizilkoyun Necropolis Area*, **Dicle Üniversitesi Mühendislik Fakültesi Mühendislik Dergisi**, **11**(3), 2020, pp. 1241–1250. DOI:10.24012/dumf.801662.

[14] J. Bródka, M. Wałek, *„The Modernist Refugium": the heritage of polish post-war residential architecture of Jerzy Ziętek's villa in Ustroń in the perspective of documentation techniques*, **International Journal of Conservation Science**, **13**(3), 2022, pp. 865–878. DOI: 10.2478/acee-2022-0027.

[15] K. Pavelka, L. Starková, K. Nováček, *Using terrestial and aerial photogrammetry in archaeology*, **International Multidisciplinary Scientific GeoConference Surveying Geology and Mining Ecology Management, SGEM**, **19**, 2019, pp. 679–688. DOI:

10.5593/sgem2019/2.2/s10.084.
[16] M.E. Atik, Z. Duran, M. Yanalak, D.Z Seker, A. Ak, *3D modeling of historical measurement instruments using photogrammetric and laser scanning techniques*, **Digital Applications in Archaeology and Cultural Heritage**, **30**, 2023, Article Number: 00286. DOI:10.1016/j.daach.2023.e00286.
[17] A. Alptekin, M. Yakar, *3D model of Üçayak Ruins obtained from point clouds*, **Mersin Photogrammetry Journal**, **3**(2), 2021, pp. 37–40. DOI:10.53093/mephoj.939079.
[18] F. Condorelli, J. Bonetto, *3D digitalization and visualization of archaeological artifacts with the use of photogrammetry and virtual reality system*, **The International Archives of the Photogrammetry, Remote Sensing and Spatial Information Sciences**, XLVIII-2-W, 2/W1-2022, 2022, pp. 51–57. DOI: 10.5194/isprs-archives-xlviii-2-w1-2022-51-2022.
[19] O.C. Wei, Z. Majid, H. Setan, M.F.M Ariff, K.M. Idris, N. Darwin, A.R. Yusoff, K. Zainuddin, *Three-dimensional recording and photorealistic model reconstruction for virtual museum application – an experience in Malaysia*, **The International Archives of the Photogrammetry, Remote Sensing and Spatial Information Sciences**, XLII-2-W9, 2/W9, 2019, pp. 763–771. DOI:10.5194/isprs-archives-xlii-2-w9-763-2019.
[20] Y. Alshawabkeh, M. El-Khalili, E. Almasri, F. Bala'awi, A. Al-Massarweh, *Heritage documentation using laser scanner and photogrammetry. The case study of Qasr Al-Abidit, Jordan*, **Digital Applications in Archaeology and Cultural Heritage**, **16**, 2020, Article Number: e00133. https://doi.org/10.1016/j.daach.2019.e00133.
[21] M. Arza-García, M. Gil-Docampo, J. Ortiz-Sanz, *A hybrid photogrammetry approach for archaeological sites: Block alignment issues in a case study (the Roman camp of A Cidadela)*, **Journal of Cultural Heritage**, **38,** 2019, pp. 195–203. DOI:10.1016/j.culher.2019.01.001.
[22] H. Khalloufi, A. Azough, N. Ennahnahi, F.Z. Kaghat, *Low-cost terrestrial photogrammetry for 3d modeling of historic sites: a case study of the Marinids'Royal Necropolis city of Fez, Morocco*, **Mediterranean Archaeology and Archaeometry**, **20**(3), 2020, pp. 257–272. DOI:10.5281/zenodo.3930412.
[23] Y.J. Hoon, S. Hong, *Three-Dimensional Digital Documentation of Cultural Heritage Site Based on the Convergence of Terrestrial Laser Scanning and Unmanned Aerial Vehicle Photogrammetry*, **ISPRS International Journal of Geo-Information**, **8**(2), 2019, Article Number: 53. DOI:10.3390/ijgi8020053.
[24] S. Del Pozo, P. Rodríguez-Gonzálvez, D. Hernández-López, J. Onrubia-Pintado, D. Guerrero-Sevilla, D. González-Aguilera, *Novel Pole Photogrammetric System for Low-Cost Documentation of Archaeological Sites: The Case Study of „Cueva Pintada"*. **Remote Sensing**, **12**(16), 2020, pp. 2644. DOI:10.3390/rs12162644.
[25] M. Vangeli, S. Lischi, G. Gattiglia, F. Sala, *Photogrammetry for 3D representation of human remains from the necropolis KR-N1 in Dhofar (Southern Oman): digital technology applied to osteo-archaeological studies*, **Archeologia e Calcolatori**, **34**(2), 2023, pp. 263–276. DOI:10.19282/ac.34.2.2023.14.
[26] I. Cârlan, B. Dovleac, *3D modelling of Arutela Roman Castrum using close-range photogrammetry*, **International Journal of Conservation Science**, **8**(1), 2017, pp. 35–42. https://www.researchgate.net/publication/316642509.
[27] A. Olszewska, S. Simpson, *Czy istnieją pogańskie piksele? Współczesna ikona Światowida i wyznaczniki jej świętości*, **Państwo i Społeczeństwo**, **4**, 2009, pp. 115–124. academica.edu.pl/reading/readMeta?page=1&uid=30351091.
[28] * * *, **Muzeum Archeologiczne w Krakowie,** https://ma.krakow.pl.
[29] M. Kowalska, *Opracowanie metodyki przetwarzania danych z naziemnego skaningu laserowego w pomiarach kontrolnych obiektów inżynierskich,* **Ph.D. Thesis,** Department of Photogrammetry, Remote Sensing and Spatial Information Systems, 2021. repo.pw.edu.pl/info/phd/WUT7606393aa3b044928c061e6611a449f4/

[30] * * *, **CloudCompare, User Manual**, 2015.
[31] U. Marmol, *Analiza algorytmów detekcji obiektów infrastruktury kolejowej na podstawie chmury punktów mobilnego skaningu laserowego*, **Archiwum Fotogrametrii, Kartografii i Teledetekcji**, **24**, 2012, pp. 211–220. bwmeta1.element.baztech-41f8b94b-a05e-49ce-aa4f-622c3789399c

Received: June 20, 2024
Accepted: November 29, 2024